Conflict-Related Theta Activity in the Midfrontal Cortex: An Electrophysiological Rodent Model for Response Conflict

Jordi ter Horst[1,2]
Supervisors: Nils Zuiderveen Borgesius[1,2], Michael X Cohen[1,2]

[1]Radboud University Nijmegen, Donders Institute for Brain, Cognition and Behaviour, The Netherlands
[2]Radboud University Medical Centre Nijmegen, Donders Institute for Brain, Cognition and Behaviour, The Netherlands

During response conflict, when a stimulus is associated with multiple responses, there is need for a mechanism that enables selection of the goal-relevant response, while suppressing a habitual response. Due to the lack of spatial and temporal precision in previous studies that tried to understand the mechanisms underlying response conflict, four male wild-type Long-Evans-Tg(TH-Cre)3.1Deis rats were trained on an adapted Simon task. After training they were implanted with a custom-made probe to record local field potentials from the midfrontal cortex during execution of the Simon task. During conflict, when the stimulus side did not match with the response side, reaction times and errors increased. Additionally, intracranial electrophysiology in the midfrontal cortex revealed that theta power (5-8 Hz) increased during conflict. This newly established electrophysiological rodent model opens up new possibilities for studying the underlying neural circuits of response conflict.

Keywords: response conflict, electrophysiology, rodent model, midfrontal cortex

Corresponding author: Jordi ter Horst; E-mail: jordi.terhorst@radboudumc.nl

During everyday life people sometimes face the problem of response conflict, a phenomenon in which an external stimulus causes an internal conflict since the stimulus is associated with multiple potential responses. In most cases of response conflict there is a habitual response that has to be prevented in order to react with the goal-relevant response. Response conflict has been studied a lot in the past using the Simon task, in which participants are asked to manually respond to a stimulus characteristic (e.g. colour) while ignoring the stimulus location. It is typically found that participants respond faster when the stimulus side corresponds with the response hand side (congruent) as compared to when the stimulus side does not correspond with the response hand side (incongruent), and erroneous responses are made more often during incongruent trials (Simon & Rudell, 1967; Simon, Hinrichs, & Craft, 1970). The effect on reaction time, known as the Simon effect, is dependent on the congruency of the previous trial (Stürmer, Leuthold, Soetens, Schröter, & Sommer, 2002; Egner, 2007). When the previous trial is incongruent, this can result in a decrease or even a reversal of the Simon effect as compared to when the previous trial is congruent.

Besides the typical effects of stimulus-response congruency on reaction times and error rates, several electrophysiological manifestations have been shown to occur during response conflict. The first one is a conflict-related power increase in the theta band (4-8 Hz) around 400 ms after cue onset, located at electrodes covering the midfrontal cortex (MFC) (Cohen & Donner, 2013; Cohen & Ridderinkhof, 2013; Nigbur, Ivanova, & Stürmer, 2011). This conflict-related theta modulation appears to be predominantly non-phase-locked to stimulus and response, meaning that ongoing endogenous theta band oscillations change in amplitude as a function of conflict, rather than being elicited by the appearance of the stimulus or the button press. In addition, non-phase-locked theta power can predict congruency and correlates positively with reaction times (Cohen & Donner, 2013). Whereas theta modulations occur around the frontal part of the midline, there are other oscillatory features that arise after conflict. Using source reconstruction, Cohen and Ridderinkhof (2013) found evidence for network shifting driven by the congruency of a trial. Whereas midfrontal theta couples with lateral prefrontal theta during incongruent trials, during congruent trials there is stimulus-contralateral parietal gamma coupling with ventrolateral frontal theta, followed by coupling between midfrontal theta and stimulus-contralateral parietal alpha. It is suggested that gamma decoupling during incongruent trials occurs to prevent the conflicting spatial location to hinder the correct response. Decreased coupling in the alpha range during incongruent trials might reflect the prevention from keeping the contralateral stimulus attended, but this seems to be unrelated to conflict resolution since this decoupling usually occurs after the response is made. Theta coupling between the MFC and lateral prefrontal cortex (LPFC) during incongruent trials probably reflects the inhibition of the incorrect response, as the amount of coupling negatively correlates with the size of the Simon effect (Cohen & Ridderinkhof, 2013).

Several cognitive models have tried to explain the mechanisms underlying response conflict, but they lack a biologically plausible mechanism for the effects that can be found (Cohen, 2014). To be able to understand how cognitive control is implemented during response conflict, and how it consecutively affects behaviour, it is necessary to monitor the underlying processes in the physical substrate. Although previous studies already took much effort in trying to capture the ongoing physiology during response conflict, they are still difficult to interpret in terms of how stimulus input step-by-step leads to response outcome.

One way to investigate the physiological processes in more detail is to measure electrophysiological signals intracranially, which gives higher spatial resolution as compared to the more common extracranial methods used in previous studies on response conflict. To measure intracranial electrophysiology, there is need for a rodent model of the Simon task, which also shows the typical effects reported in human studies. Courtière, Hardouin, Burle, Vidal, and Hasbroucq (2007) adapted the Simon task to a rat-compatible version and showed that the Simon effect is also evident in rats, as indicated by increased reaction times and more response errors when the stimulus side is not congruent with the response side. As a follow-up, Marx et al. (2012) used positron emission tomography (PET) to capture the brain areas involved in conflict processing during the adapted Simon task. Similar to human studies, they found involvement of midfrontal and premotor areas, given the increased metabolic activity after rats performed the task. Together with the work done by Courtière et al. (2007) this suggests that this rodent model is suitable for studying response conflict. However, the underlying biological processes are still unknown, since PET does not provide insight into ongoing neuronal processes while the rat is preparing a response. Especially time-frequency dynamics could use more elaboration to better understand how stimulus input consecutively results in response outcome during response conflict.

To better understand how stimulus input step-by-step leads to response outcome during response conflict, there is need for a rodent model that enables investigation of ongoing electrophysiology. In this study, rats were trained on the Simon task after which they were implanted with a custom-made probe in the MFC. As intracranial electrophysiological signals during the Simon task have never been studied before, this thesis primarily focused on conflict-related power changes in the MFC. First, typical behavioural manifestations were verified to replicate validation of this rodent model for response conflict. Second, time-frequency analysis showed conflict-related theta modulations in the MFC.

Method

Animals

Four male wild-type Long-Evans-Tg(TH-Cre)3.1Deis rats took part in this study, weighing 275-310 g before the training procedure started (Rat Resource & Research Center, Columbia, Missouri, USA). They were housed pairwise in Makrolon type III cages (UNO B.V., Zevenaar, The Netherlands) with a reversed 12-hour light-dark cycle (lights dimming at 06:30 and being off at 07:00) in a temperature- and humidity-controlled room (21 ± 2°C, 60 ± 15%). When rats weighed more than 350 g they were housed in Makrolon type IVS cages. After probe implantation, the rats were housed individually and the flat conventional cage lids were substituted with high lids to prevent implant damage. The rats had *ad libitum* access to food pellets and were restricted on water consumption except for half an hour each training and testing day. Water restriction was used because rewards during the training procedure and testing phase were given in the form of water drops. During weekends, when the rats were not trained and tested, they had *ad libitum* access to food pellets and water. Water bottles were taken away on Sundays so rats would be motivated to obtain water on the consecutive training or testing day. Weight and health were monitored on a daily basis to ensure welfare of the rats. All animal procedures were approved by the Animal Welfare Body of the Radboud University Nijmegen and the Animal Experiment Committee, according to national and international laws, to protect appropriate welfare under experimental conditions.

Materials

Training and testing sessions took place in a custom-built Skinner box (25 x 27 x 25 cm), in which one side wall contained three nose poke holes (bottom-left, bottom-centre, bottom-right), four yellow-coloured light-emitting diodes (LED; top-left, top-right, bottom-left, bottom-right), and two small loudspeakers (left, right; see Fig. 1). Each nose poke hole contained an infrared LED transmitter and receiver to continuously monitor potential poking by the rat. The left and right nose poke hole also contained an entry for a small tube in the bottom to enable provision of 50 µL water rewards, driven by solenoid pumps (The Lee Company, Westbrook, Connecticut, USA). Rats were randomly assigned to either receive sound cues (10 vs. 15 kHz) or light cues (top vs. bottom LED), and to the stimulus-response association that would lead to a reward (e.g., one of the rats was assigned to sound cues and was eventually trained to respond in the left nose poke hole if a low pitched tone (10 kHz) was presented, and in the right nose poke hole if a high pitched tone (15 kHz) was presented). The entire Skinner box was controlled by custom MATLAB software.

To record local field potentials (LFPs) in the MFC, a custom-made probe was used. The probe consisted of 30 Tungsten wires (California Fine Wire Company, Grover Beach, CA, USA) of a diameter of 50 µm eachand all were wrapped in a styrene-isoprene-styrene polymer except for the tip. The layout of the probe was designed based on the anatomy of the MFC (see Fig. 2). Before each testing session, the probe was connected to a 32-channel headstage (Omnetics, Dublin, Ireland) of which the cable went through the roof of the Skinner box, suspending onto an elastic band. The headstage cable was connected to an acquisition board (Open Ephys, Lisbon, Portugal).

Training procedure

The behavioural task on which the rats were trained was adapted from Marx et al. (2012), with the only difference that they used food pellets as a reward instead of water drops. The training procedure was also very similar to the one used by Marx et al. (2012), consisting of 1) habituation, 2) central nose poke initiation, 3) bilateral cue discrimination, 4) unilateral cue discrimination, and 5) the Simon task. All rats were handled for two weeks before the training procedure to enable the rats to get used to the experimenter and the lab environment. After handling for two weeks, all rats were put on water restriction. During the habituation phase, rats were put in the Skinner box for 30 minutes for two consecutive days, in which they received a pseudorandom bilateral cue with a fixed time interval of 10 seconds. A reward was directly given at cue onset, independent of their response. This phase helped the rats to familiarize with the Skinner box, cues, nose poke holes and rewards. In the central nose poke initiation phase, rats had to learn to initiate a trial themselves by poking in the central nose poke hole for 1.5 seconds. At the first day of this phase, poking for just a very short time was already sufficient to initiate a trial, causing the occurrence of a pseudorandom bilateral cue and an immediate reward at the associated response side. The time necessary to poke in the central nose poke hole was increased with 0.1 seconds for the next training session if the rat could initiate at least 80 trials per hour in the previous training session. When rats were able to poke for 1.5 seconds and could initiate at least 80 trials, they proceeded to the bilateral cue discrimination phase. From this phase on, rats were trained for one hour each training day for a maximum of 152 trials, and only got a reward following accurate responding. The bilateral cue discrimination phase was meant to teach each rat its stimulus-response association leading to a reward. When rats responded correctly in at least 80% of the trials in three consecutive days, they could go to the unilateral cue discrimination phase. In this phase cues were all unilateral and congruent, meaning that they were only presented at the left or right, and only presented at the side where they had to respond. This phase was meant to familiarize the rats with unilateral cues. When they responded correctly in at least 80% of the trials in three consecutive days, they went to the Simon task (see Fig. 1). In this last phase, rats were presented with congruent and incongruent unilateral cues. Rats were ready for probe implantation when they obtained an accuracy score of at least 80% in three consecutive days.

Surgical procedure

Before rats underwent surgery for probe implantation, they got *ad libitum* water access for five days. Rats were anaesthetised with 5% isoflurane in a mixture of equal parts O_2 and air and a flow rate of 1 L/min for approximately five minutes. Then, isoflurane was set to 3% to keep the animal anaesthetised during the surgery. Breathing, body temperature, O_2, and heart rate levels were monitored every hour to assess whether the isoflurane level should be adjusted. After shaving the top surface of the head, it was fixated in a stereotactic frame and cleaned with ethanol and betadine. The isoflurane flow was mounted to the stereotactic frame to ensure proper anaesthesia. Eye ointment was applied several times during the surgery to protect the eyes from drying out. Then, carprofen (Rimadyl, 0.5 mg/kg) and lidocaine (Xylocaine, 0.4 mL) were injected subcutaneously at the incision site. A midline incision was made from behind the eyes (± 3 cm in front of Bregma) to the attachment of the neck muscle (± 1 cm behind Lambda). The skull surface was cleaned with sterile cloths and bleached with 5% H_2O_2 to rough up the surface, making it easier for dental cement to stick to it later on. Then, a 0.7 mm hole was drilled, contralateral to the side of probe implantation, to enable insertion of a skull screw for the ground wire of the probe. After measuring and marking the implantation location (see Fig. 2), a craniotomy was made with a stereotactic mounted drill. A bent 27G needle was used to perform durotomy above the implantation site, after which the opening was covered with saline-soaked gelatine sponges to prevent the brain from drying out. Subsequently, the probe was carefully implanted using the stereotactic frame and Vaseline was used to cover the exposed brain surface. The ground wire coming from the probe was attached to the skull screw and covered with conductive paint. To fix and reinforce the probe, dental cement (Parkell, Edgewood, NY, USA) was applied. Eventually the skin was stitched in such a way that the rat could easily blink the eyes. Following that, isoflurane flow was turned off and the rat was removed from the stereotactic frame. The rat was put in a new clean cage on a paper towel, with a heat mat put under the cage while ensuring an unheated location in the cage for the first night. Food was provided in the form of softened and sweetened pellets, as well as a daily subcutaneous injection of carprofen (Rimadyl, 5 mg/kg), both for three consecutive days. Regular food pellets were given for the rest of the recovering period, lasting two weeks. Water was accessible *ad libitum* and weight, wound healing, and general health were monitored daily.

After this recovering period, rats were put on water restriction again to make them motivated to respond correctly during the Simon task. From this moment on intracranial electrophysiology was recorded from the MFC on a daily basis while performing the Simon task. A recording session took approximately one hour, or 152 trials if the rat was faster.

Behavioural pre-processing

All analyses were performed in MATLAB

(R2016b, The MathWorks, Inc., Natick, Massachusetts, US). For each trial, the MATLAB environment saved the congruency, response side, response correctness, reaction time (RT) and movement time (MT). RTs were defined as the time between cue onset and central nose poke release, whereas MTs were defined as the time between central nose poke release and left or right nose poke response (see Fig. 1). Only sessions with an average performance of 80% or higher were included in analyses, as an average performance of 75% could already be obtained by responding correctly in all congruent trials and guessing in incongruent trials. All trials with an RT faster than 150 ms were eliminated, as it was very likely that the rat was not attending the stimulus, or was randomly poking in one of the lateral nose poke holes. All trials with RTs exceeding two standard deviations above the median were also discarded, because it was unsure whether the rat was really engaged in these trials. Trials with incorrect responses were not included for evaluating the difference in RTs and MTs between congruent and incongruent trials. The cut-off for significance was set at p = .05.

LFP pre-processing

LFP data were acquired at 30 kHz and saved in raw format. The data were then downsampled offline at 1000 Hz and epoched in time windows between -1 and 2 seconds surrounding cue onset. Although the actual time window of interest is between -0.5 and 1 seconds, slightly broader windows were epoched to prevent edge artifacts in the time-frequency representation. Trials were visually inspected in EEGLAB (Delorme & Makeig, 2004) and manually rejected if they contained movement artifacts or other artifacts that were clearly distinguishable from true electrophysiology from the brain (see Fig. 3 for typical raw data). Independent component analysis (ICA) was used to remove components in the data that were clearly driven by non-brain sources, but were not removed if they also contained a sufficient amount of true brain-generated electrophysiological activity. Trial rejection and component removal was done blind to conditions and responses. Similar to behavioural pre-processing, all trials with incorrect responses and reaction times faster than 150 ms or slower than two standard deviations above the median were eliminated from further analyses, as well as data from sessions that had a performance lower than 80%. These pre-processing steps eventually led to rejection of 27% of the trials. For this thesis, only a randomly chosen subset of sessions from one rat was used for LFP analysis due to the time-consuming pre-processing steps.

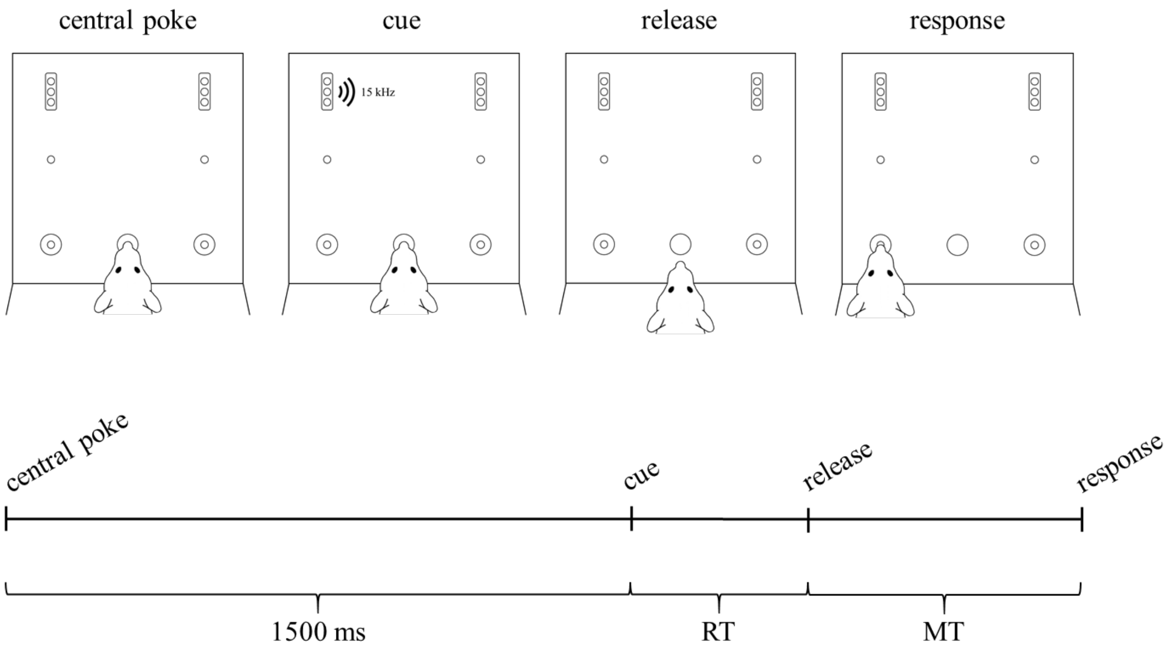

Figure 1. The Simon task adapted for rats. Rats had to initiate a trial themselves by poking in the central nose poke hole for 1500 ms. Then, a pseudorandom cue (congruent or incongruent) was presented for 300 ms, associated with a left or right reward. Reaction time (RT) was defined as the time between cue onset and central nose poke release, and movement time (MT) as the time between central nose poke release and response at either the left or right nose poke hole. Note that the cue and response side in this figure are examples.

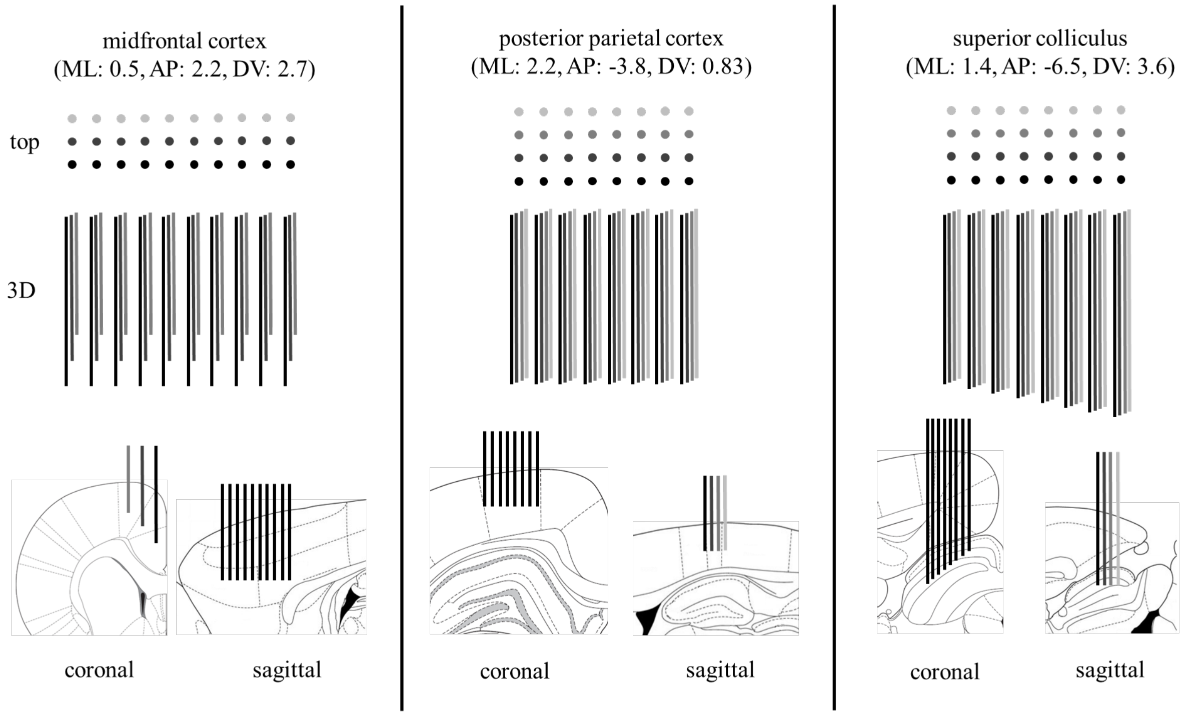

Figure 2. Probe configuration for the midfrontal cortex. The top view of the probe is depicted in the top left corner, showing the 3x10 (500x2250 µm) layout. The bottom left illustrates the probe configuration from a three-dimensional perspective, and the right half of the figure shows the intended positioning of the probe in the rat brain. The coronal slice is from the right hemisphere, and the sagittal slice is shown with the rostral side on the left. Coordinates mentioned in the top right of the figure describe the centre of the probe.

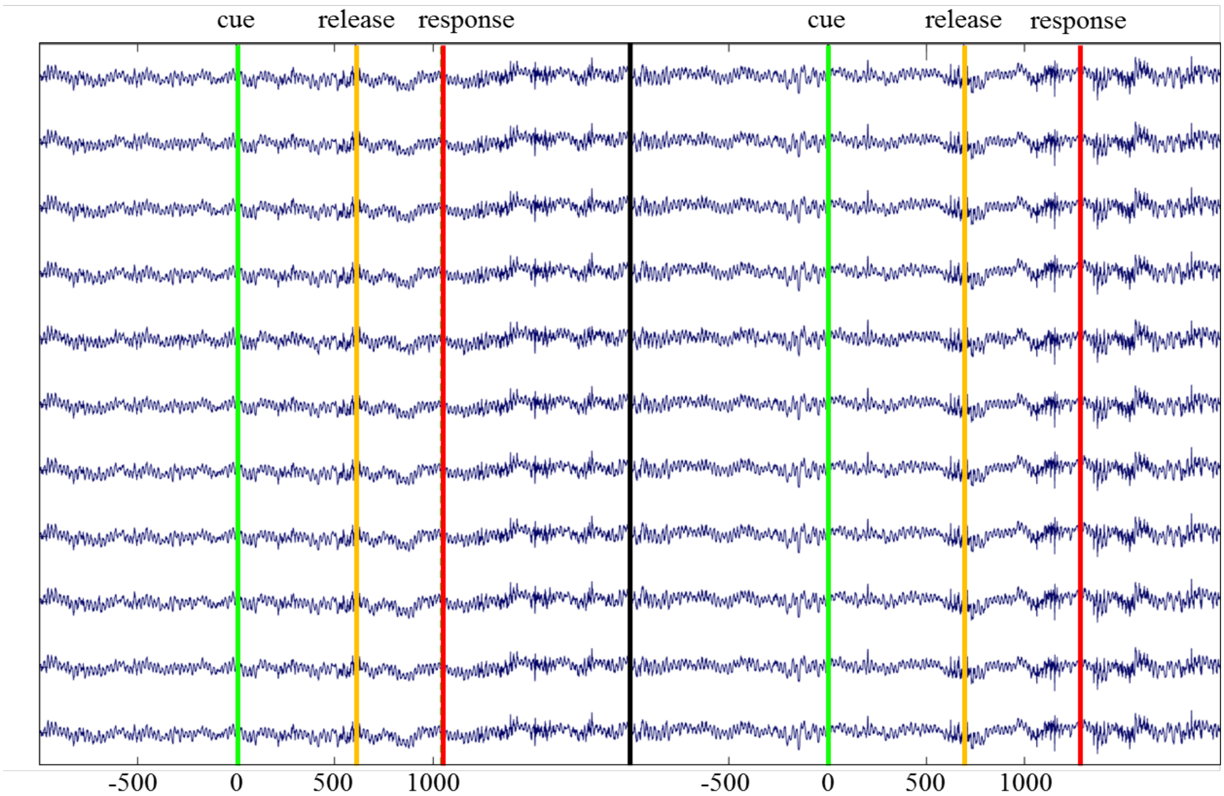

Figure 3. Epochs of typical raw data from a random selection of channels and trials, with markers indicating the cue (green), release (yellow) and response (red). Time (ms) is displayed on the x-axis and channels on the y-axis, scaled to 1500 µV for each channel.

LFP analysis

For each channel the trial data were decomposed into their time-frequency characteristics by pointwise multiplying the fast-Fourier-transformed data with the fast-Fourier-transformed complex Morlet wavelets ($e^{i2\pi tf}e^{-t^2/2s^2}$), where *t* is time, *f* is frequency (ranging from 1 to 40 in 40 logarithmically spaced steps), and *s* the width of the Gaussian for each frequency ($n/2\pi f$) with *n* reflecting the number of cycles (ranging from 3 to 8 in 40 logarithmically spaced steps). After this multiplication, the inverse fast Fourier transform was taken to obtain a complex signal from which power for each frequency at each time point could be extracted by squaring the complex signal. The result of this was then decibel power normalized ($10log10(power/baseline)$) for each frequency separately, where the baseline was picked as -500 to -200 ms before cue onset.

To test for statistically significant power changes in the MFC related to response conflict, single-trial power values for each channel, frequency and time point were extracted for permutation-based statistics. At each of the 1000 permutations, the condition label was randomly swapped on a trial-by-trial basis. The difference map between congruent and incongruent trials was computed, after which values in the difference map were transformed to z-scores. If z-scores did not exceed the critical z-value for significance, they were set to zero. After this, the biggest cluster size was stored based on which the null hypothesis distribution was eventually created. Then, the observed clusters were transformed to z-scores and set to zero if they did not exceed the cluster threshold that was based on the null hypothesis distribution of biggest cluster sizes with $p = .05$.

Results

Behavioural results

Three *t*-tests for independent samples were used for each rat with condition (congruent, incongruent) as independent variable to test whether the congruency affected reaction time, movement time, and error rate. Because electrophysiological analysis focusses on one rat, this paragraph will also focus on this rat (rat 1, red-coloured in Fig. 4 and Table 1). The statistics of the other three rats are reported in Table 1, showing effects in line with the rat reported here, or with even bigger effect sizes. Following behavioural data in human Simon tasks, RTs were slower on incongruent trials compared to congruent trials ($t(5462) = 3.34$, $p < .001$, $d = 0.09$). However, MTs did not differ depending on the congruency ($t(5347) = 1.27$, $p = .203$, $d = 0.03$). In line with the conflict-effect on RTs, the rat also made more errors on incongruent trials compared to congruent trials ($t(6041) = 2.60$, $p = .009$, $d = 0.07$).

As can be seen in Figure 4, there is a tendency for rats to have slower RTs and longer MTs if the cue is presented in the auditory domain as compared to the visual domain. However, claims cannot be made about this due to a low sample size, as it was not the primary goal to test for the effect of stimulation domain on RT. Another remarkable aspect is a low conflict effect for rat 1, which is most visible on the error rate. It is suspected that this is due to the larger amount of Simon task sessions this rat has done as compared to the other three rats, enabling this rat to be more trained to deal with response conflict. Overall, it can be concluded that the rats showed the Simon effect.

Task-related power changes

Evaluation of power dynamics averaged over conditions shows that two major task-related components were elicited, as can be seen in the upper plots in Figure 5. Around 300 ms after cue onset there was an increase in alpha power (~7-14 Hz), as well as an increase in high-delta power around 500 ms after cue onset (~2.5-4.5 Hz). Post-hoc data driven *t*-tests were used to identify whether these alpha and delta power increases were affected by conflict, by averaging the power values within each window for each trial, for each channel separately. The alpha window was defined between 250-900 ms and 7-14 Hz, whereas the delta window was defined between 350-700 ms and 2.5-4.5 Hz (see contours in upper plots of Fig. 5). None of the channels captured significant differences in the average alpha or delta power between congruent and incongruent trials (alpha: $t(175) = –0.05$ - 1.06, $p = .292$ - $.977$, $d = –0.01$ - 0.16; delta: $t(175) = 0.10 – 0.70$, $p = .482$ - $.922$, $d = 0.01 – 0.11$).

Conflict-related power changes

As illustrated with black-coloured contours in the bottom plots of Figure 5, cluster-based permutation testing revealed several windows that were statistically significant ($p < .05$, uncorrected for multiple comparisons) between congruent and incongruent trials. As expected, there was a conflict-related increase in theta power (5-8 Hz) around 250 ms after cue onset, which is before the average reaction time (congruent trials: 597 ms, incongruent trials: 667 ms). An even stronger conflict-related power increase was observed in the beta-band (12-30 Hz) around 750 ms following cue onset, which is shortly after the average reaction time. Although all contoured windows did not survive correction for multiple comparisons, it is interesting to see how conflict-related midfrontal theta and beta are distributed over the channels in the MFC. Therefore, the average power within the conflict-related theta and beta contour was computed for each channel separately. As can be seen in Figure 6, visual inspection shows there was no smooth pattern transition in power across the channel layout for both conflict-related theta and beta, except that there was more theta power in frontal channels, and more beta power in posterior channels. A post-hoc t-test indeed showed that the 15 frontal channels displayed significantly more theta power as compared to the 15 posterior channels ($t(28) = 3.63$, $p = .001$, $d = 1.32$). Similarly, but in the opposite direction, there was more beta power in the 15 posterior channels as compared to the 15 frontal channels ($t(28) = -2.13$, $p = .042$, $d = -0.78$). A Spearman's correlation showed that conflict-related theta and beta power did not correlate with each other ($r = -.05$, $p = .784$).

Total power versus non-phase-locked power

Subtracting the phase-locked signal (ERP, event-related potential) from the time-series data for both conditions separately did not result in clearly visible changes in the time-frequency domain, as illustrated with the left versus right column of Figure 5. This indicated that the majority of task-related and conflict-related power changes were due to amplitude modulations of ongoing endogenous oscillations, not being time-locked to cue onset. As there was no clear difference in total power versus non-phase-locked power, all reported analyses were performed with the total power series data.

Relation between theta power and reaction time

To investigate the possible relationship between theta power and reaction time during congruent and incongruent trials, theta power between 5 and 8 Hz was extracted for each channel separately from 100 to 350 ms after cue onset. This window was chosen based on the contoured conflict-related theta window (see lower plots in Fig. 5). Power values within this time window were averaged for each trial and correlated with the RT in that same trial. Although 29 out of 30 MFC channels showed the expected positive correlation during incongruent trials, Spearman's correlation was not significant for any of the 30 channels in the probe ($r = -0.01$ - 0.11, $p = .288$ - $.967$). Contrary to incongruent trials, 28 out of 30 MFC channels showed negative correlations during congruent trials, but none of the Spearman's correlations were significant ($r = -0.14$ - 0.01, $p = .226$ - $.955$).

Discussion

Towards a rodent model for studying neural circuits of response conflict

Table 1.

Statistics on reaction time, movement time and error rate for each individual rat. Every rat colour in the left column corresponds to the colours in Figure 4. Note that the degrees of freedom reported here are much larger than the degrees of freedom reported in electrophysiological analyses, as only a randomly chosen subset of sessions from one rat was used for electrophysiological analyses due to the time-consuming pre-processing steps.

	Reaction time	Movement time	Error rate
Rat 1 sound cues	$t(5462) = 3.34$, $p < .001$, $d = 0.09$	$t(5347) = 1.27$, $p = .203$, $d = 0.03$	$t(6041) = 2.60$, $p = .009$, $d = 0.07$
Rat 2 sound cues	$t(1144) = 3.48$, $p < .001$, $d = 0.21$	$t(1101) = 2.30$, $p = .022$, $d = 0.14$	$t(1334) = 6.80$, $p < .001$, $d = 0.37$
Rat 3 light cues	$t(2007) = 8.83$, $p < .001$, $d = 0.39$	$t(2014) = 2.35$, $p = .019$, $d = 0.11$	$t(2291) = 8.47$, $p < .001$, $d = 0.35$
Rat 4 light cues	$t(2556) = 16.52$, $p < .001$, $d = 0.65$	$t(2581) = 0.04$, $p = .970$, $d = 0.00$	$t(2943) = 6.84$, $p < .001$, $d = 0.25$

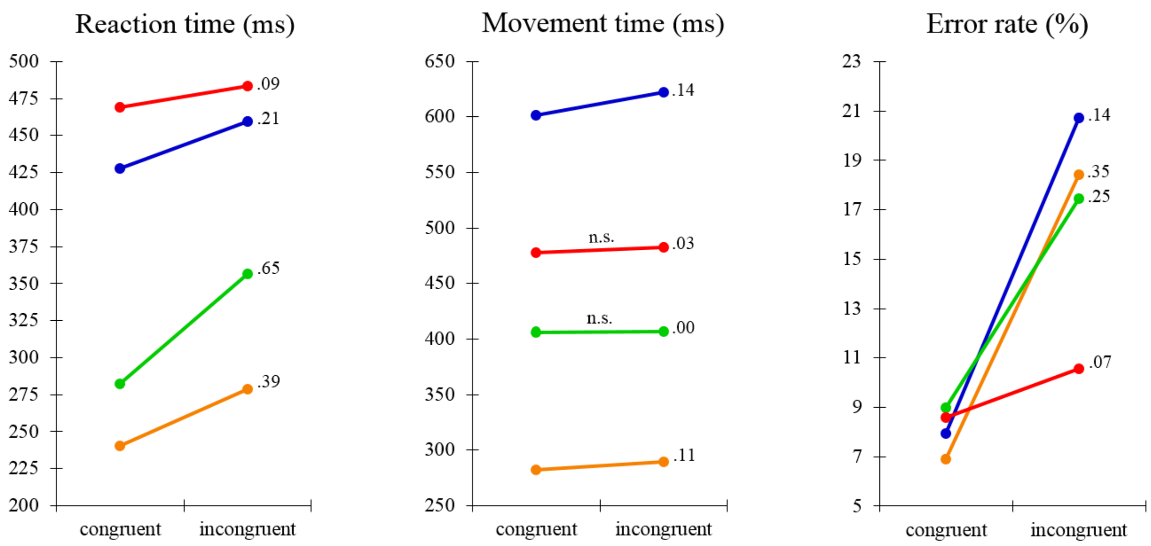

Figure 4. Mean reaction time, movement time and error rate depicted for congruent and incongruent trials, for each individual rat in a separate colour (rats coloured red and blue received auditory cues, rats coloured green and yellow received visual cues). The numbers next to each line represent effect sizes (Cohen's d). Non-significance is indicated by n.s. on top of the line. The cut-off for significance was set at p = 0.05.

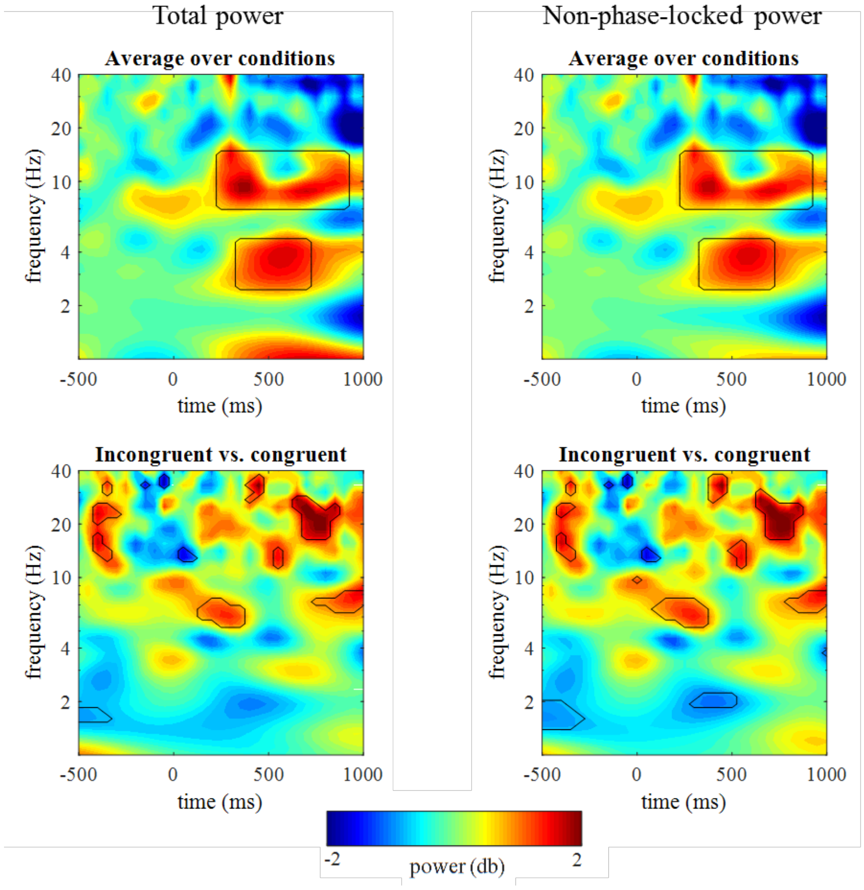

Figure 5. Time-frequency plots for the total power (left) and non-phase-locked power (right) relative to cue onset. The upper two plots show the average task-related power over both congruent and incongruent trials, whereas the bottom two plots show conflict-related power changes. Contours in the top two plots surround the windows of interest for post-hoc analysis. Contours in the bottom two plots indicate significant ($p < .05$) windows of conflict-related power changes. None of these contours survived correction for multiple comparisons. Note that y-axes are logarithmically scaled. Data is from a typical MFC channel.

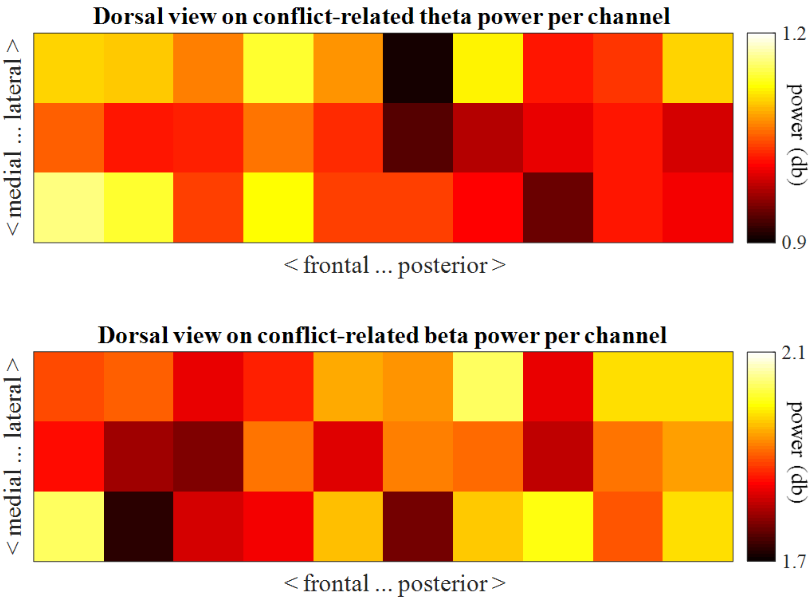

Figure 6. Dorsal view on the 3x10 channel layout of the MFC probe with conflict-related theta (top) and beta (bottom) power shown for each channel separately. Note the difference in scaling of power values between the top and bottom plot.

Previous studies in humans on response conflict lacked anatomical precision, due to the use of extracranial electrophysiology. On the other hand, the animal studies that were already executed by Courtière et al. (2007) and Marx et al. (2012) did not provide the temporal precision needed to study the neural circuits underlying response conflict. The current study aimed to validate an intracranial electrophysiological rodent model for response conflict, to enable researchers in the future to study the mechanisms in the physical substrate with both anatomical and temporal precision. Comparable with human response conflict, this study shows that the Simon effect in rats manifests in both the visual and auditory domain, and that there is an increase in theta power during conflict in the MFC. This rodent model opens up possibilities to study response conflict in more detail, and specifically, study the role of ongoing electrophysiological processes within and between different brain regions during response conflict and resolution.

Conflict-related theta activity in the midfrontal cortex

The contrast between congruent and incongruent trials revealed several changes in power, of which one frequency band was most prominent before the average reaction time. Comparable with human response conflict, conflict-related theta power increases after cue onset, is predominantly non-phase-locked, and occurs before the average reaction time. This theta power increase is relatively stronger in the anterior half of the MFC probe, suggesting that this power change has its origin in more frontal regions in the MFC. Although histology should give a definite answer about the exact coordinates of the channels, and thus the brain region in which the theta increase is most prominent, it might well be that the frontal channels of the MFC probe were located close to or in the prelimbic cortex (see left panel in Fig. 2).

The prelimbic cortex in rats is thought to be associated with response selection, response planning, reward anticipation, and working memory (Emmons, Ruggiero, Kelley, Parker, & Narayanan, 2016; Seamans, Floresco, & Phillips, 1995; Seamans, Lapish, & Durstewitz, 2008; Vertes, 2004). Lesions to the prelimbic cortex result in impaired performance on tasks in which multiple responses are optional (Delatour & Gisquet-Verrier, 1996). Given the projections that originate in the prelimbic cortex, this region is comparable with the dorsolateral prefrontal cortex (DLPFC) in humans (Seamans et al., 2008; Vertes, 2004). In human studies, the (D)LPFC is found to be associated with conflict resolution, potentially through attentional biasing or action inhibition, by theta-coupling between the MFC and LPFC (Cohen & Ridderinkhof, 2013; Cavanagh, Cohen, & Allen, 2009; Kim, Chung, & Kim, 2013; Swart et al., 2018). Because it is very plausible that theta in the current study originates from the prelimbic cortex, these lines of evidence suggest that conflict-related theta increases in the current study are homologous to the conflict-related theta increases found in human studies.

Activity in other frequency bands

Beta power increased during conflict after the average RT. Contrary to conflict-related theta power, this beta power is relatively stronger in the posterior half of the MFC probe. These posterior channels were probably located near to or in the cingulate cortex (see left panel in Fig. 2). The cingulate cortex is associated with a multitude of cognitive functions, such as selective attention, response flexibility, and effort- and reward-guided decision making (Cowen, Davis, & Nitz, 2012; Kim, Wasserman, Castro, & Freeman, 2016; Porter, Hillman, & Bilkey, 2019; Seamans et al., 1995). Inactivation of the cingulate cortex with muscimol impairs selective attention during the presence of a distractor stimulus (Kim et al., 2016), and the majority of neurons in the anterior part of the cingulate cortex code for specific amounts of effort (Porter et al., 2019). However, there is a lack of studies describing beta power fluctuations in this region during cognitive tasks in rats, which makes it difficult to grasp which of these potential processes it might reflect. Another possibility is that this beta power reflects a response inhibition process through synchronisation in motor-related areas. The striatum is located very close to the posterior half of the MFC probe (< 2 mm), and it is well known that response inhibition processes are accompanied by striatal beta synchronisation, which eventually suppresses motor cortex output (Aron, Herz, Brown, Forstmann, & Zaghloul, 2016; Eagle & Robbins, 2003; Wessel et al., 2016; Zavala et al., 2018). Although local field potentials are thought to reflect the sum of current fluctuations from a very small area surrounding the probe, volume conduction still enables probes to pick up signals from neighbouring tissue up to 6 mm away (Kajikawa & Schroeder, 2011). It is not unlikely that the increase in conflict-related beta power reflects the inhibition of an initiated movement towards the incorrect nose poke hole, so the correct movement direction can become dominant in order to obtain a reward.

Across conditions increases in alpha and high-delta power were found, both appearing after cue onset. Increases in frontal alpha and delta power during cognitive tasks in humans and non-human primates are associated with a variety of cognitive functions such as attention, working memory, inhibition, and mental calculation (Bonnefond & Jensen, 2012; Harmony, 2013; Jensen & Bonnefond, 2013). However, translating primate-based findings to rodent electrophysiology might be inaccurate to do. Concerning rat studies, some researchers argue for the role of the MFC in auditory detection. A study by Herzog, Salehi, Bohon, and Wiest (2014) showed increased alpha activity after auditory cue onset, and another study found spiking activity related to the detection of auditory targets in the MFC, but not related to movement direction (Bohon & Wiest, 2014). In addition to increased alpha power after auditory cues, it has been previously found that auditory cues are followed by increases in midfrontal delta power if the cue is followed by a reward after a delay period, suggesting that post-cue delta power reflects cue-driven reward anticipation (Emmons et al., 2016). It might very well be that the increase in high-delta in the current study reflects something similar, as the rat could always expect a reward after moving to the correct lateral nose poke hole. Indepth investigation of the potential relationship between post-cue alpha/high-delta power and behaviour is needed to elucidate whether it plays a role in response conflict.

Limitations

One of the benefits of using intracranial electrophysiology during task execution is to investigate the relationship between trial-by-trial variations in power dynamics and behavioural measures. However, the current study failed to find a relationship between these two measures, as theta power and RT did not correlate significantly in both congruent and incongruent trials. Interestingly, during incongruent trials almost all channels showed the expected direction, namely higher theta power during trials with slower RTs. On the other hand, during congruent trials almost all channels showed the opposite direction, namely higher theta power during trials with faster reaction times. In human response conflict, Cohen and Donner (2013) found a positive correlation in both congruent and incongruent trials, which raises the question why the direction of effect in the current study is not identical across congruent and incongruent trials. It might be the case that midfrontal theta during congruent trials does not reflect conflict, but something like an attentional or motivational process. However, caution should be taken about the cause of this heterogeneity to prevent over-interpretation of these non-significant correlations.

Another limitation of the current study is the amount of data included for electrophysiological analysis. Only a total of 244 trials were included, leaving 177 trials after pre-processing, which might have caused underpowered statistical analyses. However, this study demonstrates the richness of data collected with intracranial electrophysiology during a behavioural task, as it enables a wide range of analyses to be performed to better understand the underpinnings of response conflict and cognitive control in general.

Conclusions and future directions

In conclusion, this study successfully shows that this rodent model is well suited for studying the electrophysiological mechanisms underlying response conflict. Typical behavioural manifestations of response conflict in rats are evident in both the auditory and visual domain, showing increased reaction times and more errors during conflict. In addition, intracranial electrophysiology shows that theta power increases during conflict, originates from anterior parts of the MFC, and occurs after cue onset.

To better understand the circuitry underlying response conflict, future analyses could focus on functional connectivity between the MFC and other brain regions during conflict processing. Besides this, investigating the anatomical connections between them will shed light on the potential flow of information from stimulus to response. When these circuits are better known, interference with optogenetics can provide causal evidence about the dynamics that drive conflict processing and resolution. A point of attention in this whole process is to study response conflict in multiple sensory domains, to elucidate which components are specific to visual or auditory conflict, and which components are shared and therefore more fundamental in response conflict.

References

Aron, A. R., Herz, D. M., Brown, P., Forstmann, B. U., & Zaghloul, K. (2016). Frontosubthalamic circuits for control of action and cognition. *The Journal of Neuroscience, 36,* 11489–11495.

Bohon, K. S., & Wiest, M. C. (2014). Role of medio-dorsal frontal and posterior parietal neurons during auditory detection performance in rats. *PloS ONE, 9,* 1–12.

Bonnefond, M., & Jensen, O. (2012). Alpha oscillations serve to protect working memory maintenance against anticipated distracters. *Current Biology, 22,* 1969–1974.

Cavanagh, J. F., Cohen, M. X., & Allen, J. J. B. (2009). Prelude to and resolution of an error: EEG phase synchrony reveals cognitive control dynamics during action monitoring. *The Journal of Neuroscience, 29,* 98–105.

Cohen, M. X. (2014). A neural microcircuit for cognitive conflict detection and signaling. *Trends in Neurosciences, 37,* 480–490.

Cohen, M. X., & Donner, T. H. (2013). Midfrontal conflict-related theta-band power reflects neural oscillations that predict behavior. *Journal of Neurophysiology, 110,* 2752–2763.

Cohen, M. X., & Ridderinkhof, K. R. (2013). EEG source reconstruction reveals frontal-parietal dynamics of spatial conflict processing. *PloS ONE, 8,* 1–14.

Courtière, A., Hardouin, J., Burle, B., Vidal, F., & Hasbroucq, T. (2007). Simon effect in the rat: A new model for studying the neural bases of the dual-route architecture. *Behavioural Brain Research, 179,* 69–75.

Cowen, S. L., Davis, G. A., & Nitz, D. A. (2012). Anterior cingulate neurons in the rat map anticipated effort and reward to their associated action sequences. *Journal of Neurophysiology, 107,* 2393–2407.

Delatour, B., & Gisquet-Verrier, P. (1996). Prelimbic cortex specific lesions disrupt delayed-variable response tasks in the rat. *Behavioral Neuroscience, 110,* 1282–1298.

Delorme, A., & Makeig, S. (2004). EEGLAB: An open source toolbox for analysis of single-trial EEG dynamics including independent component analysis. *Journal of Neuroscience Methods, 134,* 9–21.

Eagle, D. M., & Robbins, T. W. (2003). Inhibitory control in rats performing a stop-signal reaction-time task: Effects of lesions of the medial striatum and d-amphetamine. *Behavioral Neuroscience, 117,* 1302–1317.

Egner, T. (2007). Congruency sequence effects and cognitive control. *Cognitive, Affective, & Behavioral Neuroscience, 7,* 380–390.

Emmons, E. B., Ruggiero, R. N., Kelley, R. M., Parker, K. L., & Narayanan, N. S. (2016). Corticostriatal field potentials are modulated at delta and theta frequencies during interval-timing task in rodents. *Frontiers in Psychology, 7,* 1–9.

Felsen, G., & Mainen, Z. F. (2008). Neural substrates of sensory-guided locomotor decisions in the rat superior colliculus. *Neuron, 60,* 137–148.

Harmony, T. (2013). The functional significance of delta oscillations in cognitive processing. *Frontiers in Integrative Neuroscience, 7,* 1–10.

Herzog, L., Salehi, K., Bohon, S., & Wiest, M. C. (2014). Prestimulus frontal-parietal coherence predicts auditory detection performance. *Journal of Neurophysiology, 111*, 1986–2000.

Ignashchenkova, A., Dicke, P. W., Haarmeier, T., & Their, P. (2004). Neuron-specific contribution of the superior colliculus to overt and covert shifts of attention. *Nature Neuroscience, 7,* 56–64.

Jensen, O., & Bonnefond, M. (2013). Prefrontal alpha- and beta-band oscillations are involved in rule selection. *Trends in Cognitive Sciences, 17,* 10–12.

Kajiwaka, Y., & Schroeder, C. E. (2011). How local is the local field potential? *Neuron, 72,* 847–858.

Kim, C., Chung, C., & Kim, J. (2013). Task-dependent response conflict monitoring and cognitive control in anterior cingulate and dorsolateral prefrontal cortices. *Brain Research, 1537,* 216–223.

Kim, J., Wasserman, E. A., Castro, L., & Freeman, J. H. (2016). Anterior cingulate cortex inactivation impairs rodent visual selective attention and prospective memory. *Behavioral Neuroscience, 130,* 75–90.

Krauzlis, R. J., Liston, D., & Carello, C. D. (2004). Target selection and the superior colliculus: Goals, choices and hypotheses. *Vision Research, 44,* 1445–1451.

Marx, C., Lex, B., Calaminus, C., Hauber, W., Backes, H., Neumaier, B., ... Endepols, H. (2012). Conflict processing in the rat brain: Behavioral analysis and functional µPET imaging using [^{18}F] fluorodeoxyglucose. *Frontiers in Behavioral Neuroscience, 6,* 1–12.

Nigbur, R., Ivanova, G., & Stürmer, B. (2011). Theta power as a marker for cognitive interference. *Clinical Neurophysiology, 122,* 2185–2194.

Porter, B. S., Hillman, K. L., & Bilkey, D. K. (2019). Anterior cingulate cortex encoding of effortful behavior. *Journal of Neurophysiology, 121,* 701–714.

Posner, M. I., Walker, J. A., Friedrich, F. J., & Rafal, R. D. (1984). Effects of parietal injury on covert orienting of attention. *The Journal of Neuroscience, 4,* 1863–1874.

Seamans, J. K., Floresco, S. B., & Philips, A. G. (1995). Functional differences between the prelimbic and anterior cingulate regions of the rat prefrontal cortex. *Behavioral Neuroscience, 109,* 1063–1073.

Seamans, J. K., Lapish, C. C., & Durstewitz, D. (2008). Comparing the prefrontal cortex of rats and primates: Insights from electrophysiology. *Neurotoxicity Research, 14,* 249–262.

Simon, J. R., Hinrichs, J. V., & Craft, J. L. (1970). Auditory S-R compatibility: Reaction time as a function of ear-hand correspondence and ear-response-location correspondence. *Journal of Experimental Psychology, 86,* 97–102.

Simon, J. R., & Rudell, A. P. (1967). Auditory S-R compatibility: The effect of an irrelevant cue on information processing. *Journal of Applied Psychology, 51,* 300–304.

Stürmer, B., Leuthold, H., Soetens, E., Schröter, H., & Sommer, W. (2002). Control over location-based response activation in the Simon task: Behavioral and electrophysiological evidence. *Journal of Experimental Psychology: Human Perception and Performance, 28,* 1345–1363.

Swart, J. C., Frank, M. J., Määttä, J. I., Jensen, O., Cools, R., & den Ouden, H. E. M. (2018). Frontal network dynamics reflect neurocomputational mechanisms for reducing maladaptive biases in motivated action. *PloS Biology, 16,* 1–25.

Vertes, R. P. (2004). Differential projections of the infralimbic and prelimbic cortex in the rat. *Synapse, 51,* 32–58.

Wessel, J. R., Ghahremani, A., Udupa, K., Saha, U., Kalia, S. K., Hodaie, M., ... Chen, R. (2016). Stop-related subthalamic beta activity indexes global motor suppression in Parkinson's disease. *Movement Disorders, 31,* 1846–1853.

Whitlock, J. R. (2017). Posterior parietal cortex. *Current Biology, 27,* 681–701.

Yang, F. C., Jacobsen, T. K., & Burwell, R. D. (2017). Single neuron activity and theta modulation in the posterior parietal cortex in a visuospatial attention task. *Hippocampus, 27,* 263–273.

Zavala, B., Jang, A., Trotta, M., Lungu, C. I., Brown, P., & Zaghloul, K. A. (2018). Cognitive control involves theta power within trials and beta power across trials in the prefrontal-subthalamic network. *Brain, 141,* 3361–3376.